EFFECT OF MODULE INCLINATION ANGLE ON AIR GAP MEMBRANE DISTILLATION

David E. M. Warsinger[1], Jaichander Swaminathan[1], John H. Lienhard V[1*],

[1]Rohsenow Kendall Heat Transfer Laboratory, Department of Mechanical Engineering Massachusetts Institute of Technology, 77 Massachusetts Avenue, Cambridge MA 02139-4307 USA

ABSTRACT

Air gap membrane distillation (AGMD) experiments were performed with varied temperature and varied module inclination angles to characterize the effect of module angle on permeate production and thermal performance. While AGMD is potentially one of the most energy efficient membrane distillation configurations, transport resistances in the air gap typically dominate the thermal performance, resulting in degraded permeate production. Tilting the module away from vertical offers the opportunity to manipulate the condensate layer and its associated thermal resistance. In this study, we report experiments on varying module tilt angle performed with a flat plate AGMD module under fully characterized heat and mass transfer conditions. Numerical modeling is also performed to better understand the experimental results. The tests indicated that the AGMD system behaves as a "permeate gap", or flooded membrane distillation system for declined and extremely inclined positions. A key finding relevant to all AGMD systems is that at highly negative tilt angles (more than 30 degrees), condensate may fall onto the membrane causing thermal bridging and increased permeate production. Near vertical and positive tilt angles (<15 degrees from vertical) show no significant effect of module tilt on performance, in line with model predictions.

KEY WORDS: Condensation, Mass transfer, Membrane Distillation, AGMD, Desalination, Tilt Angle, Thermal Efficiency

1. INTRODUCTION

Membrane distillation (MD) is an emerging thermally-powered desalination technology with unique advantages at small scales, and potential to reach superior efficiencies compared to existing desalination technologies. In an MD system, a hot, saline solution with a high vapor pressure flows across a hydrophobic membrane which selectively allows water vapor to pass through but not liquid water or dissolved salts. Pure water diffuses through the membrane and is condensed and collected on the other side. Due to its scalability and low maintenance, most applications to date for this emerging technology have been for small installations, some driven by solar thermal power [1]. Recent papers have suggested that MD can theoretically provide superior efficiencies to all other thermal desalination technologies, including Multi-Stage Flash (MSF) and Multi-Effect Distillation (MED) [2][3], although actual test results have shown more modest thermal performance [4]. Several configurations have been designed for MD, including the most commonly, Direct Contact Membrane Distillation (DCMD) and Air Gap Membrane Distillation (AGMD), as well as Vacuum Membrane Distillation (VCMD), and Sweeping Gas Membrane Distillation (SGMD) [5]. Of these configurations, it has been shown that AGMD has higher potential for superior thermal efficiencies [6].
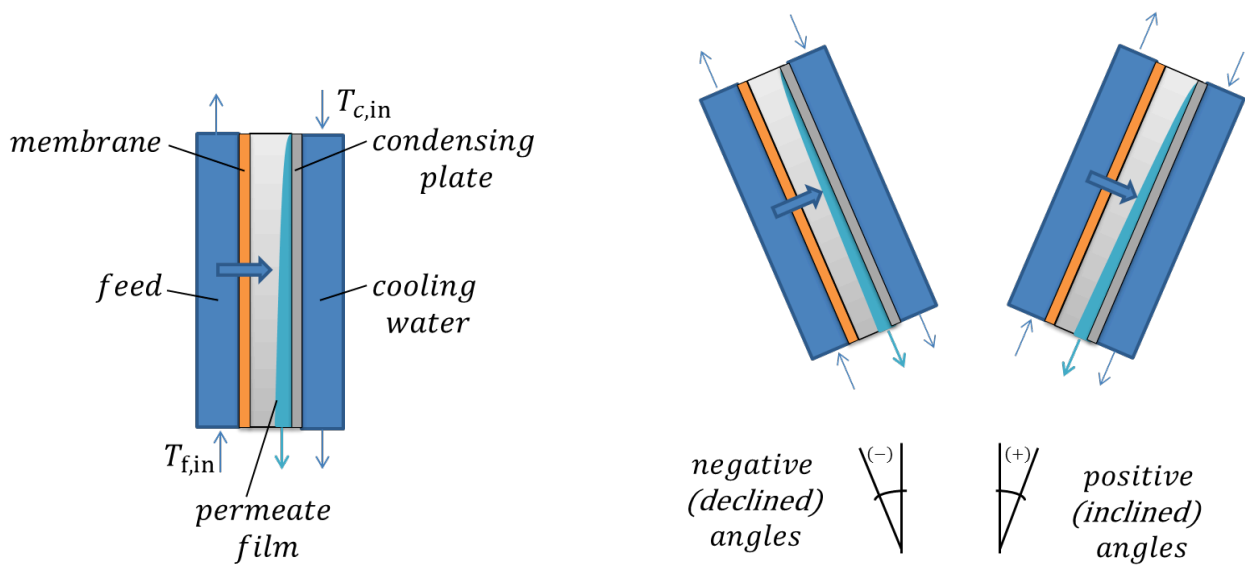
*Corresponding Author: lienhard@mit.edu

Fig 1. AGMD at varied angles

AGMD includes a saline feed, a hydrophobic membrane, an air gap behind the membrane, and a condensing surface beyond the air gap. Various configurations have been designed, including flat sheet designs, a tubular configuration with concentric cylinders, hollow fiber modules and spiral wound modules [5]. This study examines the effect of varying the tilt angle of AGMD modules, which is primarily applicable to flat plate configurations, but also to tubular and spiral wound systems. Flat plate systems are among the most common due to their ease of manufacturing and assembly, and are used in experimental systems as well as commercial modules such as those produced by MEMSYS [7].

In AGMD systems with small air gaps, an important phenomenon that can occur during operation is flooding and associated thermal bridging. Flooding occurs when the permeate production rate exceeds the rate of condensate removal from the air gap. This effect reduces mass transfer resistance, tending to increase permeate production rate, but it also increases heat loss from and temperature polarization in the feed channel as heat is conducted directly through the water from the membrane to the cooling plate. Thermal bridging may also occur at small, localized regions at which water falls from the condenser onto the membrane surface for declined tilt angles, if local bridging of the membrane and condensation plate occurs. As this phenomenon is unsteady and localized, it cannot be readily modelled in the generic model.

Module tilt angle has been studied in many condensation technologies. While the vertical module orientation has been the norm in AGMD studies [8], horizontal module orientation has also been used in some cases [9], which we define here as angles approaching positive 90° from vertical as seen in Fig. 1 above. While relatively unimportant in other configurations such as DCMD, where tilt angle only has hydrostatic effects, the module tilt angle affects droplet flow and film thickness on the condenser surface in AGMD systems. The literature generally lacks experiments at other angles, although 45 degrees has been examined for DCMD, not AGMD, configurations in experiments using bubbles to encourage turbulence [10]. To the authors' knowledge, the present paper is the first detailed experimental and theoretical analysis of the effect and optimization of tilt angle on an AGMD process, and the first to examine declined angles for AGMD.

2. EXPERIMENT DESIGN

To analyze the effect of module tilt angle, experiments were performed on an AGMD test bed under fully characterized heat and mass transfer operating conditions. This system consists of two controlled fluid flow loops which serve a tilt-enabled central testing module.

2.1 Apparatus Design

As seen in Fig. 2, a hot saline loop circulates feed water past one side of the membrane, and a separate cold side loop chills the condensing plate. Both loops use tanks for thermal storage to stabilize temperature, and include pumps, flow meters, and temperature controllers.
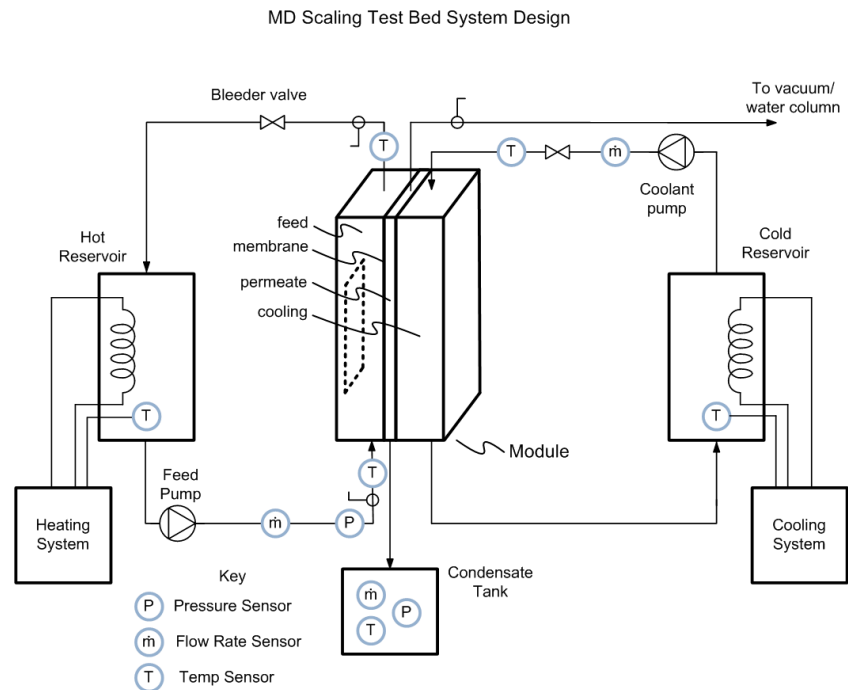
MD Scaling Test Bed System Design

Fig 2. Experiment setup

As seen in Fig. 3, the module consists of a series of plates for the various channels. The feed and cooling channels are made of polycarbonate plates with machined channels. A polycarbonate spacer separates the membrane and aluminum condensing plate.
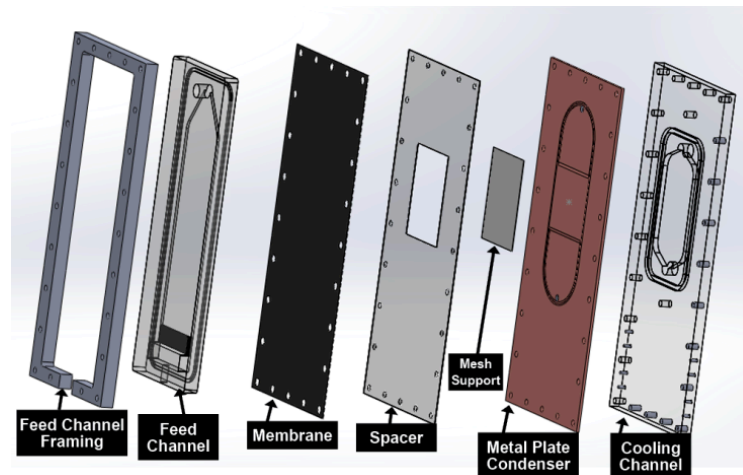
Fig 3. AGMD Module Plate design

The channels can be described by their internal dimensions, where the length is the streamwise dimension from inlet to outlet and runs vertically in the above diagrams, the width runs horizontally, and the depth is the shallow dimension cut into each plate. While the feed plate is 35 cm long, only 16 cm is exposed to the membrane, with the region preceding it ensuring a fully developed turbulent flow beneath the active membrane region.

Table 1. Parameters for AGMD module experiments

	Feed Channel	Air Gap	Cooling Channel
Length	35 cm	16 cm	16 cm
Width	12 cm	12 cm	12 cm
Depth	4 mm	1 mm	10 mm
Pressure	1.4 atm	1 atm	NA
Temperature	40°C - 70°C	10°C - 40°C	10°C - 50°C

The membranes used are hydrophobic Immobilon-PSQ membranes. Although originally designed for protein binding, they have good characteristics for MD and have also been used in previous AGMD studies [6]. The membranes have an average pore size of 0.2 μm, a maximum pore size of 0.71 μm, and a porosity of 79.2%. A membrane coefficient of B = 1.6×10^{-7} s/m is used to characterize the permeability in the numerical models [1]. A fine mesh spacer is used to keep the membrane's flat shape; McMaster part number 9265T51. A course mesh spacer with most horizontal wires removed maintains the air gap width; McMaster part number 9275T65 [11].

3. NUMERICAL MODELING

3.1 Modeling Methods and Feed Channel Modeling

The theoretical performance of the AGMD system at varied angles is estimated using numerical modeling techniques with Engineering Equation Solver (EES) [12], which is an iterative equation solver with several thermodynamic property functions built into it. A one-dimensional modeling approach is followed in which the temperatures and flow rates vary along the length of the module. The width of the module is assumed to be long so that the effect of the walls is negligible and properties are constant along this direction. In the depth direction, the boundary layers and associated resistances are taken into account, and the difference between the temperature and concentration for the bulk stream and at the membrane interface is evaluated using suitable heat and mass transfer coefficients.

The primary modeling calculations involve mass and energy conservation equations applied to each of the module sections: the feed channel, the air gap, and the coolant channel. Each section is coupled with suitable transport equations. A detailed description of the overall modeling methodology applied for the case of vertical module orientation is given by Summers et al. [1]. The heat and mass transfer coefficients are determined through the Nusselt and Sherwood numbers evaluated within each stream. The equations are solved using EES, and the number of computational cells was progressively increased to 120, by which point the results were seen to be grid independent.
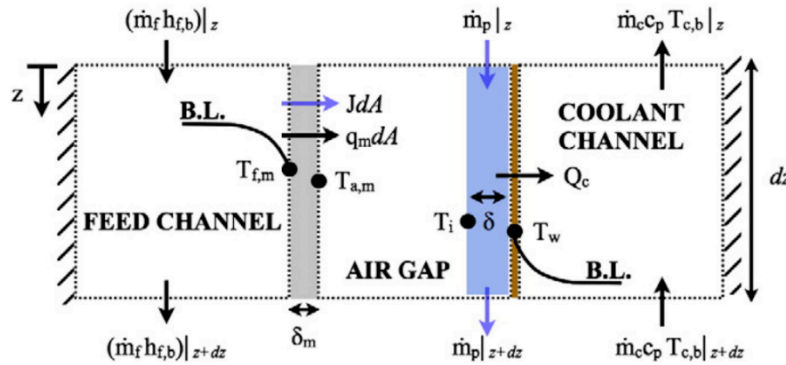

Fig. 4 An integral control volume of a computational cell for the AGMD model from [6].

The mass flow of water vapor is given by the membrane characteristic equation (Eq. 1) and depends on the water vapor pressure on either side of the membrane. The mass flow rate in the feed stream reduces correspondingly.

$$J = B \times (P_{vap,f,m} - P_{vap,a,m}) \tag{1}$$

Here J is the permeate flux, B is the membrane permeability, $P_{vap,f,m}$ is the vapor pressure on the feed side surface of the membrane, and $P_{vap,a,m}$ is the vapor pressure on the air gap side surface of the membrane.

3.2 Air Gap and Condensing Channel Modeling

The air gap modeling is especially important since the transport resistances in this region significantly affect the AGMD module performance. Varying the tilt angle of the module can affect the process only through

5

physical changes in this region. Typically, a spacer mesh is placed in this region to prevent the flexible membrane from collapsing onto the condensation surface. Like most other numerical models of the AGMD module, the spacer is not explicitly considered and a free air gap is modeled.

During operation, part of the membrane is pressed down into the gaps in the mesh and the effective air gap depth is reduced. For modeling purposes, the membrane is considered to be flat for simplicity. The effective depth of the air gap is therefore taken at a value lower than the design value in order to account for this effect.

No condensation or heat transfer through the polypropylene mesh spacer is considered, as the conductivity of the mesh is very low, limiting both conduction through it, and keeping it at a higher temperature than the condensation plate, limiting condensation on the mesh. The water vapor flux entering the air gap diffuses through the air layer to reach the film and condense. The air layer is less than 1 mm in depth and hence any convection effects are ignored.

The flux through the membrane is a function of the vapor fraction at the interface on the air gap side. The vapor diffuses to the water interface from this interface. The diffusion is governed by binary mass diffusion as described in Lienhard and Lienhard [13].

$$\frac{J_m}{M_w} = \frac{c_a D_{w-a}}{d_{gap} - \delta} \, ln\left(1 + \frac{x_i - x_{a,m}}{x_{a,m} - 1}\right) \tag{2}$$

Here, J_m is the flux through the membrane, M_w is the molecular weight of water, c_a is the concentration of air, D_{w-a} is the diffusivity of water in air, d_{gap} is the air gap width, x_i is the water mole fraction at the liquid-vapor interface, and $x_{a,m}$ is the water mole fraction at the membrane interface.

The thickness of the air gap increases as more liquid condenses into it. By mass conservation, assuming no shear at the liquid-air interface, the rate of growth of the film can be evaluated as

$$\delta_{i+1}^3 = \delta_i^3 + \frac{3 J_i \, dA \, v_{f,i}}{g \cos \theta \left(\rho_f - \rho_g\right) w} \tag{3}$$

where δ_i is the condensation film thickness, dA is the differential of area, $v_{f,i}$ is the fluid kinematic viscosity, g is the gravitational constant, ρ_f is the fluid density, ρ_g is the combined air and water vapor density, and w is the width [14].

Note that the denominator here has $\cos\theta$ to account for the angle of inclination. When the module is vertical, $\theta = 0°$. The formula is used for angles as high as $85°$, since the evaluated film thickness is still smaller than the air gap thickness. The heat of condensation is conducted across the film, through the aluminum wall, and into the coolant liquid.

3.3 Modeling Inputs

The numerical model takes the following inputs: geometry of the experimental setup including the length, width, and depth of each of the channels; hot water flow rate and temperature as it enters the module; and cold water flow rate and temperature at module inlet.

3.4 Effect of Module Tilt Angle

6

Fig. 5 shows the effect of tilt angle on flux in the model. The permeate production rate at a given module inclination is normalized with respect to the flux at vertical orientation and the ratio is plotted with respect to inclination angle. With all other conditions remaining the same, the thickness of the condensate film is affected by angle (Eq. 3). With a thicker film, the effective diffusion length (d_{gap} minus δ) for water vapor is reduced, and hence the flux increases (Eq. 2). This effect is independent of whether the module tilt angle is in the positive or negative direction.

An increase of around 4% is possible at very large module tilt angles as a result of the film becoming thicker. Figure 5 shows that this increase is higher for cases with lower cold side temperatures since viscosity of the film is higher and hence the film rolls off the surface slower. This small increase does not include the effects of thermal bridging or flooding.
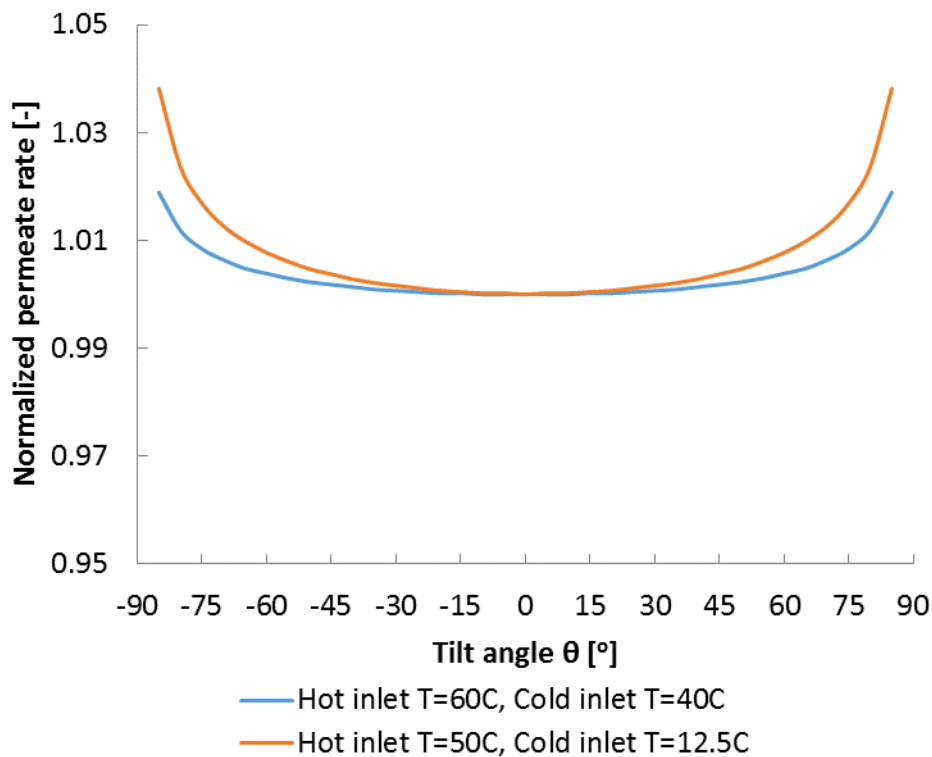

Fig. 5 Effect of module tilt angle on flux predicted by model.

4. METHODOLOGY

4.1 Experimental Methodology

The measured permeate production rates, adjusted for temperature variability, are presented. The hot side inlet and cold side inlet temperatures were set and maintained using temperature controllers during experiment operation. The hot side temperature in this experiment varies by ±0.2 °C over the course of an experiment; and on the cold side, the temperature controller, which actuates a coolant flow valve, achieves temperature control of ±0.5 °C around the set-point temperature. Between experiments at different angles,

the average inlet temperatures of the streams can change. The difference in average temperature on the feed side is at most 0.4°C and on the cold side it is at most 1°C. While Fig. 5 shows the relatively minute effect of tilt angle on flux, the stream temperatures have a much larger influence on flux. This is especially true because vapor pressure, which is the driving force for MD mass transfer, is an exponential function of temperature. In order to separate the effect of angle, the variability caused by small changes in average inlet temperatures must be identified and removed.

Using the corresponding average inlet temperature and flow rate conditions at each of the tilt angles, flux is estimated using the EES model for a vertical module operating under those conditions. The measured flux for the AGMD experimental system at vertical orientation was between 150-250 l/m²day depending on the type and thickness of the air gap spacer used in the particular test. The measured permeate production rates are scaled by multiplying by vertical module flux obtained from EES at the same temperature conditions divided by the experimentally obtained flux at 0° tilt angle. The scaled experimental fluxes are then each divided by scaled flux at 0°. The ratio obtained is called the normalized permeate rate and will have a value of unity at 0° tilt angle. At other tilt angles, the deviation from unity would indicate the relative change in flux that results from tilting the apparatus if other conditions were to remain exactly the same.

4.2 Uncertainty Quantification

Uncertainty analysis was performed within the EES code to account for uncertainties in numerically predicted flux as a result of uncertainties in measured temperatures and flow rates of the hot and cold streams. The overall uncertainty in flux was generally dominated by temperature variations. While the hot side temperature has a larger impact on flux, the absolute uncertainty in cold side temperature is higher, so that both affect overall uncertainty. The uncertainty in actual temperature measurements was estimated conservatively as the standard deviation in temperature recorded during the experiment plus the maximum measurement uncertainty of ±0.2°C for the thermistors used.

Experimentally, the flux is determined over a period of 10-15 minutes by subtracting the final water mass from the initial water mass and dividing by the total elapsed time. Each measurement is carried out at time intervals of about 5 seconds by the data acquisition system. Hence a time measurement uncertainty of 10 seconds is considered. A conservative time error was used to account for variability in permeate drop collection from the apparatus. The measurement uncertainty on the mass scale is ±0.1g. In order to account for both the initial and final readings, an uncertainty of ±0.2g is considered for the total water mass collected.

5. EXPERIMENTAL RESULTS

5.1 Effect of Angle on Permeate Flux

The experiments and modeling showed a minimal effect for small inclination angles on permeate flux. Very large angles, however, did produce a substantial increase in permeate production rate. This result is further supported by theoretical analysis of the relationship between the film thickness δ and the mass transfer resistance in the air gap and flux. The main parameter of interest is the permeate production rate; as the end product, permeate flux indicates the performance of the fixed size AGMD system with fixed top and bottom temperatures of the system. While energy efficiency of the system is also important, our apparatus does not incorporate energy recovery at the condenser, and is not intended for energy consumption studies.
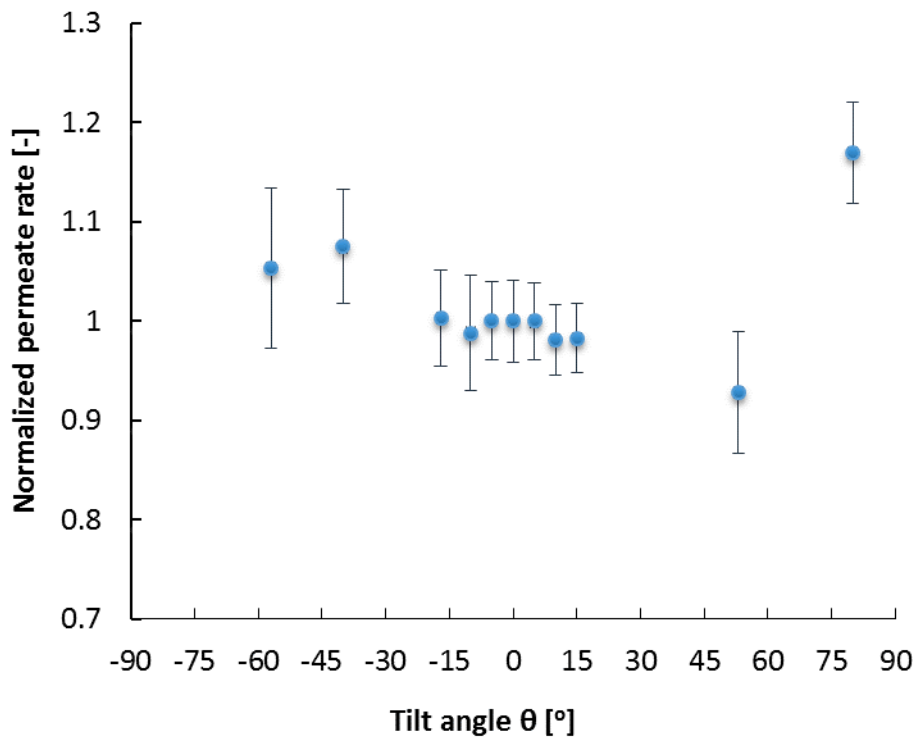
Fig. 6 Effect of module tilt angle on permeate production: $T_{f,in} \approx 50°C$, $T_{c,in} \approx 12.5°C$

Figure 6 shows the normalized permeate flow rate vs. tilt angle. The normalized permeate flow rate is the permeate flow rate for the given angle normalized for temperature changes and divided by the permeate flow rate for vertical module orientation (0°). In Fig 6., MD was performed at moderate temperatures with a high temperature difference, ΔT, between condensate and feed streams and a very low condensate temperature. Permeate flux remained relatively stable but increased at extreme angles, both for negative and positive positions. The large ΔT and very low cold side temperature caused a relatively high permeate flux. The data show a substantial jump in permeate flux at 85°, which is attributed to air gap flooding. For this nearly horizontal case, the role of gravity in draining the film is substantially diminished (c.f., Eq. 3). Additionally, for the low condenser temperature of 12.5° C, the viscosity of liquid water is roughly twice the value in later trials at 30°C, also contributing somewhat to a thicker condensate film.
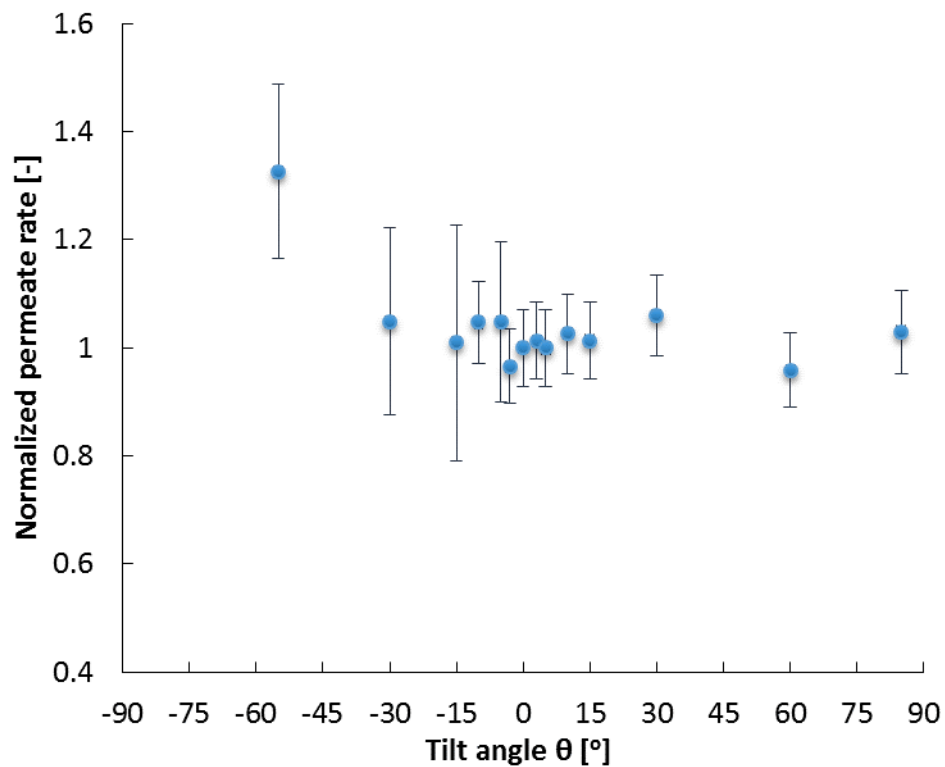
Fig. 7 Effect of module tilt angle on permeate production: $T_{f,in} \approx 60°C$, $T_{c,in} \approx 40°C$.

Figure 7, for a trial at significantly higher temperature than Fig. 6, shows that angle played a small role in positive and moderately negative angles, but that flux increased significantly at very large negative angles. This may be indicative of thermal bridging at relatively small negative angles such as -30°, rather than flooding, and a tendency to flood as the module tilt angle furhter increases and approaches -60°.

Since it is almost universally observed that thermal bridging or other effects of module tilt angle variation are effectively absent at low tilt angles, subsequent trials reduced the number of angles considered in the low angle range.
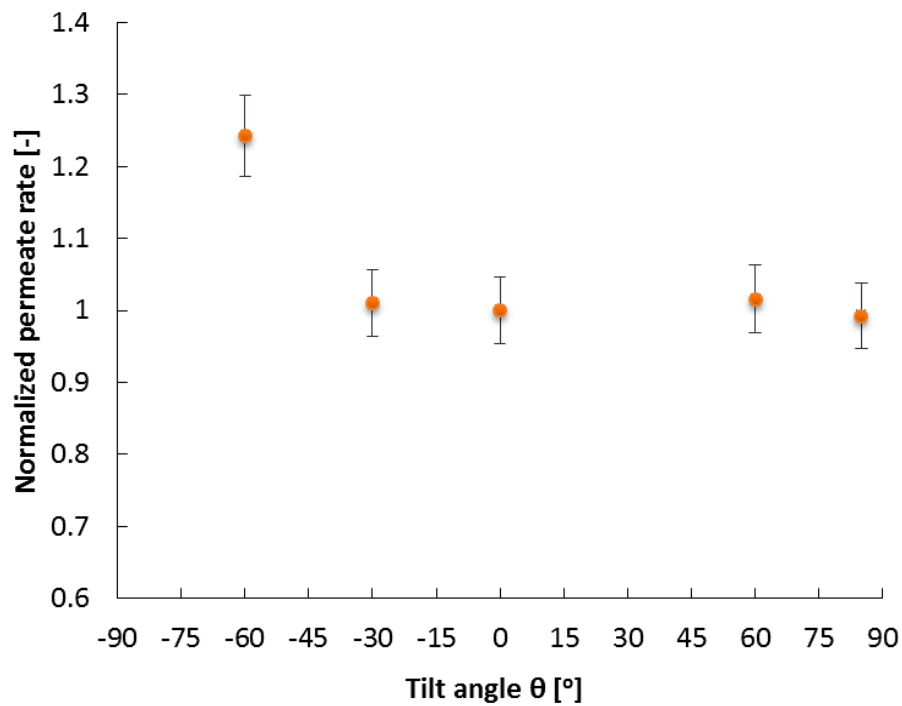
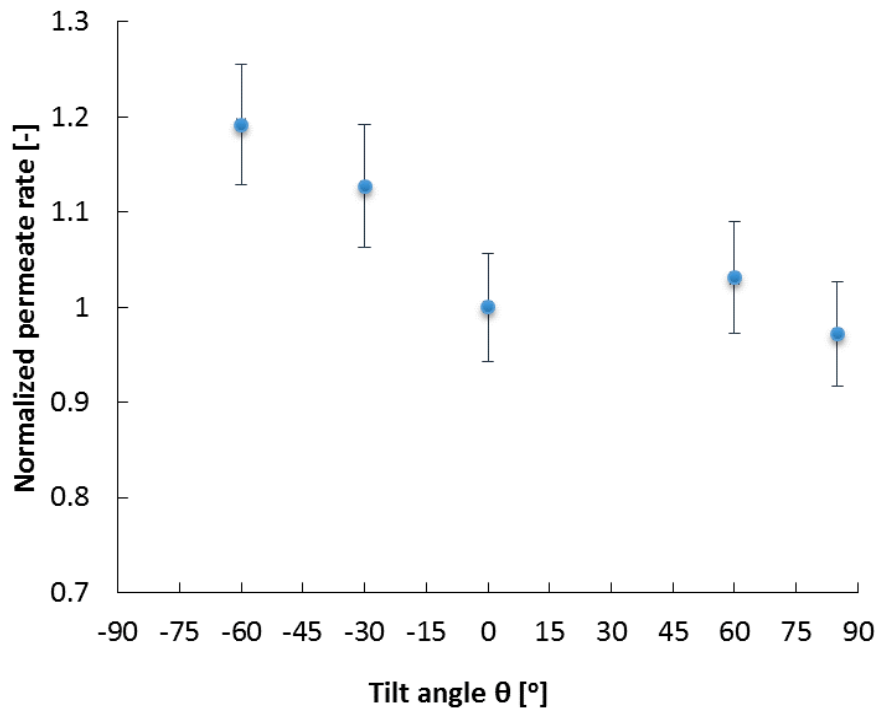**Fig. 8** Effect of module tilt angle on permeate production: Smaller air gap. $T_{f,in} \approx 50°C$, $T_{c,in} \approx 20°C$.

Fig. 9 Effect of module tilt angle on permeate production: Smaller air gap. $T_{f,in} \approx 60°C$, $T_{c,in} \approx 40°C$.

11

To further investigate the hypotheses of thermal bridging and flooding, additional trials were performed for a smaller effective air gap thickness two thirds the original thickness, using only one spacer mesh instead of two (Figs. 8 and 9). While the absolute value of permeate production rate was higher for these cases due to the reduction in effective air gap size and a corresponding decrease in diffusion length for water vapor, the relative effect of tilt angle on flux remains similar. At small negative angle and even at large positive angles, the flux remains constant. At -60°, flux increases significantly. In some cases, the effect of thermal bridging can be discerned at angles as low as -30°. Thus, these observations suggest that changes in effective air gap thickness do not have a major impact on the induction of thermal bridging effects at various tilt angles in AGMD. Notably, the higher temperature trial experienced relatively significant thermal bridging starting at an angle of only -30°, indicating a temperature dependence on risk for thermal bridging.
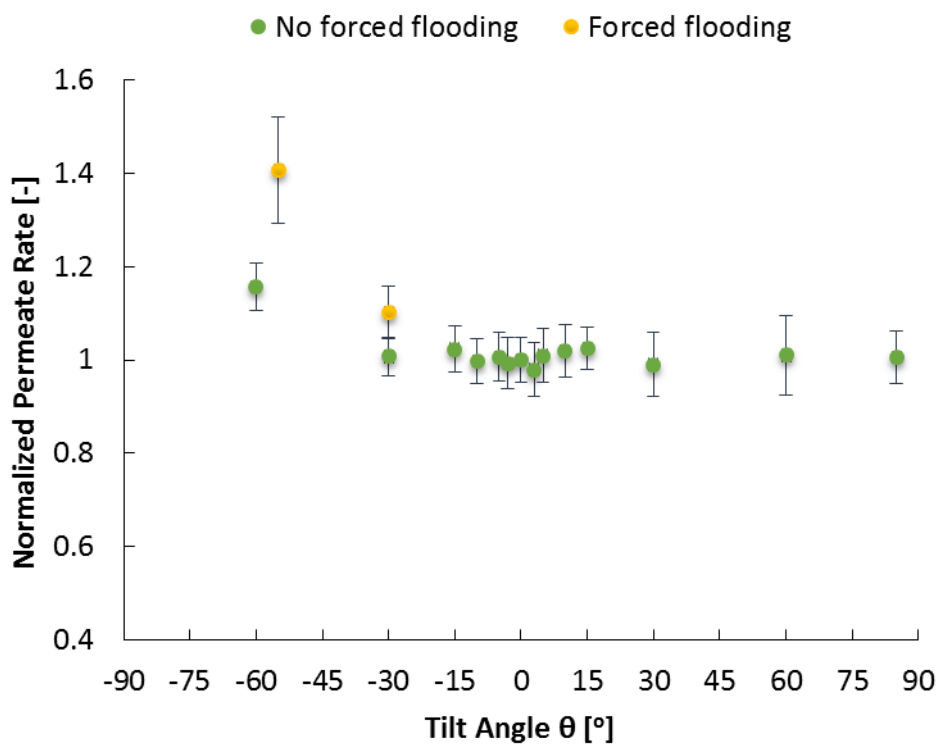

Fig. 10 Effect of module tilt angle on permeate production: Comparison with modified experiment where hydrostatically forced flooding is avoided. $T_{f,in} \approx 50°C$, $T_{c,in} \approx 20°C$

An additional trial was performed with hydrostatically forced flooding, where the permeate outlet was at a larger height than some parts of the module, thereby partial filling the air gap with liquid water. At low negative angles ($\sim$ -30°C), partial flooding begins occuring; whereas when the angle is decreased further ($\sim$ -60°C), almost the entire active membrane area is beneath the outlet and hence filled with water. Identical experiments were also performed where care was taken to avoid hydrostatically forced flooding over the active membrane area even at extreme negative angles. The results showed that forced flooding, where the entire air gap is filled with liquid water produced significantly higher permeate flux (Fig. 10). In the tests for which forced flooding was avoided, one can see that even at -30°, the permeate production rate does not change ralative to the vertical baseline. Only at higher negative angles we see an increase in relative flux, but

the extent of increase is smaller than the case of forced flooding, pointing to the possibility of water falling back onto the membrane from the condensation plate and related local theral bridging. This further demonstrates that both flooding and thermal bridging are possibilites in AGMD at high inclinations and that the relative increase in flux is affected greatly by the extent of thermal bridging.

5.2 Thermal Bridging Hypothesis

The thermal bridging may occur if fluid falls from the condensing plate onto the membrane itself, forming a liquid bridge across the local air gap. This phenomenon is not captured by the numerical model. Thermal bridging is particularly likely in the case of negative tilt angles and hence the experimental flux results are asymmetric about the 0° orientation. As the mass transfer resistance is dominated by the air gap width, this phenomena should be easily observed by an increase in permeate flux at declined angles. Our initial hypothesis was that bridging could occur even at small negative angles. In the experimental data, however, we see no such change in permeate flux at small negative angles, indicating a lack of thermal bridging. The key insight is that thermal bridging is not a concern at vertical and near vertical angles for the air gap and spacer dimensions considered here.

An explanation for the why fluid does not fall onto the MD membrane even at negative inclinations may be obtained by the considering the hydrophobicity or hydrophilicity of the surface on which the fluid flows. The aluminum condensing surface is hydrophilic: typical aluminum condensing surfaces have contact angles around 5° [15]. Meanwhile, MD membranes are hydrophobic. Thin films of water can remain on the underside of inclined hydrophilic surfaces up to very high angles of inclination [16, 17, 18]. Additionally, in small gaps where droplets can easily exceed the size of the gap, droplets on the hydrophobic surface may touch and be reabsorbed into the film on the hydrophilic condensing plate. Therefore, large tilt angles, which favor thicker liquid films, may be required before thermal bridging effects occur.

6. CONCLUSIONS

The experimental and theoretical results indicate that moderate angles of inclination only had a minor effect on permeate flux, except at high angles where it was quite significant. Permeate flux varied by less than 5% within inclination angles of ±15°, but flux increased significantly as angles approached ±90°, in some cases rising by more than 40%.

The results indicate AGMD's susceptibility to two conditions in which liquid water spans the air gap, flooding and thermal bridging. Flooding, occurring when permeate production was rapid enough to fill the air gap with permeate, is a risk at large temperature differences across the air gap, at small gap sizes, and at very high inclined or declined angles. Flooding occurs primarily at very high inclined or declined angles.

The second condition, thermal bridging, occurs at high declined angles, for which condensate detaches from the laminar film on the condenser plate and makes contact with the hot membrane surface. This condition occurred more readily than flooding at declined angles, but was not observed for angles less than 30° off vertical. Results suggest that thermal bridging and flooding are likely to occur earlier, at smaller negative inclination angles, in systems that have lower air gap thickness.

While in many cases flooding and thermal bridging may reduce thermal efficiency, in single pass systems with limited size or lacking energy recovery, the increased permeate production from high incline angles

with flooding or thermal bridging is often desirable, as more pure water is produced under the same cycle top and bottom temperature conditions.

ACKNOWLEDGMENT

NOMENCLATURE

B	membrane permeability	(s/m)	MW	Molecular Weight	(g/mol)
d_{gap}	air gap width	(mm)	δ	film thickness	(m)
h_{fg}	latent heat of vaporization	(J/kg)	ξ	porosity	(%)
J	flux	$(kg/m^2 s)$			

REFERENCES

[1] E. K. Summers and J. H. Lienhard V, "A novel solar-driven air gap membrane distillation system," *Desalination and Water Treatment*, pp. 1–8, July 2012.

[2] J. Gilron, L. Song, and K. K. Sirkar, "Design for Cascade of Crossflow Direct Contact Membrane Distillation," *Industrial & Engineering Chemistry Research*, vol. 46, pp. 2324–2334, Apr. 2007.

[3] F. He, J. Gilron, and K. K. Sirkar, "High water recovery in direct contact membrane distillation using a series of cascades," *Desalination*, vol. 323, pp. 48–54, Sept. 2013.

[4] G. Zaragoza, A. Ruiz-Aguirre, E. Guillen-Burrieze, D. Alarcon-Padilla, and J. Blanco-Galvez, "Experimental comparison of different prototypes of solar energy driven membrane distillation systems," in *Proceedings of the 2013 IDA World Congress on Desalination and Water Reuse*, 2013.

[5] A. Alkhudhiri, N. Darwish, and N. Hilal, "Membrane distillation: A comprehensive review," *Desalination*, vol. 287, pp. 2–18, Feb. 2012.

[6] E. K. Summers, H. a. Arafat, and J. H. Lienhard, "Energy efficiency comparison of single-stage membrane distillation (MD) desalination cycles in different configurations," *Desalination*, vol. 290, pp. 54–66, Mar. 2012.

[7] K. Zhao, W. Heinzl, M. Wenzel, S. Büttner, F. Bollen, G. Lange, S. Heinzl, and N. Sarda, "Experimental study of the memsys vacuum-multi-effect-membrane-distillation (V-MEMD) module," *Desalination*, vol. 323, pp. 150–160, 2013.

[8] G. L. Liu, C. Zhu, C. S. Cheung, and C. W. Leung, "Theoretical and experimental studies on air gap membrane distillation," *Heat and Mass Transfer*, vol. 34, pp. 329–335, Nov. 1998.

[9] A. Alkhudhiri, N. Darwish, and N. Hilal, "Produced water treatment: Application of air gap membrane distillation," *Desalination*, pp. 46–51, 2013.

[10] G. Chen, X. Yang, R. Wang, and A. G. Fane, "Performance enhancement and scaling control with gas bubbling in direct contact membrane distillation," *Desalination*, vol. 308, pp. 47–55, Jan. 2013.

[11] McMaster-Carr, "Chemical-resistant polypropylene mesh, part number 9275t65."

[12] S.A.Klein, "Engineering equation solver version 9."

[13] J. H. Lienhard V and J. H. Lienhard IV, *A Heat Transfer Textbook Fourth Edition*. Dover Publications, Inc, 2011.

[14] A. Mills, *Heat Transfer 2nd Edition*. Prentice Hall, 1998.

[15] J. Bernardin, I. Mudawar, C. Walsh, and E. Franses, "Contact angle temperature dependence for water droplets on practical aluminum surfaces," *International Journal of Heat and Mass Transfer*, vol. 40, no. 5, pp. 1017–1033, 1997.

[16] H. R. Nagendra, "Effect of inclination on laminar film condensation," *Applied Scientific Research*, vol. 28, pp. 261–277, 1973.

[17] J. A. Howarth, G. Poots, and D. Wynne, "Laminar film condensation on the underside of an inclined flat plate," *Mechanics Research Communications*, vol. 5, no. 6, pp. 369–374, 1978.

[18] B. J. Chung and S. Kim, "Film condensations on horizontal and slightly inclined upward and downward facing plates," *Heat Transfer Engineering*, vol. 29, pp. 936–941, 2008